



# Methane flux from living tree stems in a northern conifer forest

Christian Hettwer · Kathleen Savage · Jonathan Gewirtzman ·  
Roel Ruzol · Jay Wason · Hinsby Cadillo-Quiroz · Shawn Fraver

Received: 7 April 2025 / Accepted: 14 July 2025 / Published online: 7 August 2025  
© The Author(s) 2025

**Abstract** Methane ( $\text{CH}_4$ ) is the second-largest contributor to human-induced climate change, with significant uncertainties in its terrestrial sources and sinks. Tree stems play crucial roles in forest ecosystem  $\text{CH}_4$  flux dynamics, yet much remains unknown regarding the environmental drivers of fluxes. We

measured  $\text{CH}_4$  flux from three tree species (*Picea rubens*, *Tsuga canadensis*, *Acer rubrum*) along an upland-to-wetland gradient at Howland Research Forest, a net annual sink of  $\text{CH}_4$ , in Maine USA. We measured fluxes every two weeks and at three heights from April to November 2024 to capture a range of environmental conditions. Tree species influenced  $\text{CH}_4$  flux more than any of the environmental variables considered. Among environmental variables, soil moisture was the most important driver of  $\text{CH}_4$  flux, and our models suggested a significant interaction between soil moisture and soil temperature, such that the effect of higher soil moisture was greater at warmer soil temperatures. We determined a “break-point” in soil moisture along the upland-to-wetland gradient at  $\sim 60\%$  volumetric water content, above which  $\text{CH}_4$  flux rates increased dramatically. All stems measured were net  $\text{CH}_4$  sources throughout the sampling period, with rare, isolate measurements of minimal uptake. The magnitude of flux varied by species: red maple stems were the largest emitters ( $1.946 \pm 5.917 \text{ nmol m}^{-2} \text{ s}^{-1}$ , mean  $\pm$  SD), followed by red spruce ( $0.031 \pm 0.065$ ) and eastern hemlock ( $0.016 \pm 0.027$ ). This study highlights the contribution of these species to ecosystem  $\text{CH}_4$  fluxes. Our results establish the sensitivity of stem flux rates to projected increases in regional precipitation and temperature, potentially shifting the site from a net  $\text{CH}_4$  sink to a source.

---

Responsible Editor: Stephen D. Sebestyen

C. Hettwer (✉) · R. Ruzol · J. Wason · S. Fraver  
School of Forest Resources, University of Maine, Orono,  
ME 04469, USA  
e-mail: christian.hettwer@maine.edu

R. Ruzol  
e-mail: roel.ruzol@maine.edu

J. Wason  
e-mail: jay.wason@maine.edu

S. Fraver  
e-mail: shawn.fraver@maine.edu

K. Savage  
Woodwell Climate Research Center, Falmouth, MA 02540,  
USA  
e-mail: savage@woodwellclimate.org

J. Gewirtzman  
School of the Environment, Yale University, New Haven,  
CT 06511, USA  
e-mail: jonathan.gewirtzman@yale.edu

H. Cadillo-Quiroz  
School of Life Sciences, Arizona State University, Tempe,  
AZ 85287, USA  
e-mail: hinsby@asu.edu

**Keywords** Forest carbon cycle · Forested wetlands · Howland research forest · Trace gas biogeochemistry

## Introduction

Methane ( $\text{CH}_4$ ) emissions are the second largest contributor to human-induced climate change behind carbon dioxide ( $\text{CO}_2$ ) emissions. With a radiative forcing that may be 120 times that of  $\text{CO}_2$  immediately after emission,  $\text{CH}_4$  has a direct impact of roughly 20% of climate forcing since 1750 (Saunois et al. 2016). However, uncertainties regarding the magnitude of  $\text{CH}_4$  emissions (sources) and uptake (sinks) from terrestrial ecosystems limit our understanding of the role of  $\text{CH}_4$  in the global carbon cycle. Projections range from 150 to 274 Tg  $\text{CH}_4$  year $^{-1}$  for wetland emissions, and 20 to 45 Tg  $\text{CH}_4$  year $^{-1}$  for terrestrial ecosystem uptake (Saunois et al. 2020; Liu et al. 2020). These uncertainties limit our ability to model changes in  $\text{CH}_4$  flux, such as source–sink transitions, under a changing climate (Reeburgh 2006; Kirschke et al. 2013).

In terrestrial systems, most  $\text{CH}_4$  flux research has focused on soils, as they are thought to be the dominant biotic sink for atmospheric  $\text{CH}_4$  in upland conditions and the dominant source in wetlands (Saunois et al. 2020). However, recent research has shown that tree stems also contribute to net  $\text{CH}_4$  sink-source dynamics in upland forests (Warner et al. 2017). In terrestrial wetlands, stem flux could be largely attributable to soil-derived  $\text{CH}_4$ , which is transported through the roots and vascular tissues in wetland trees (Rusch and Rennenberg 1998; Pangala et al. 2015), and emissions from tree stems may account for as much as 20% of total temperate wetland ecosystem  $\text{CH}_4$  emissions (Gauci et al. 2010). In upland forests, most studies have observed net  $\text{CH}_4$  emissions from tree stems (Pitz and Megonigal 2017; Wang et al. 2016; Flanagan et al. 2021). However, methanogenic and methanotrophic bacteria can exist within stem tissue and on bark surfaces of trees, resulting in emission and uptake, respectively, across various soil conditions (Putkinen et al. 2021; Jeffrey et al. 2021) with direction and magnitude of net fluxes to the atmosphere remaining an area of active research (Barba et al. 2019; Gauci et al. 2024).

Further, much remains unknown regarding the environmental factors most important in driving

tree  $\text{CH}_4$  flux rates and directions. Many studies have shown soil moisture, temperature, and stem height as key predictors of  $\text{CH}_4$  flux from tree stems, with flux increasing under higher moisture and temperature conditions but decreasing at higher stem heights (Machacova et al. 2013; Maier et al. 2018). However, other studies have found these factors to explain only 7–11% of flux variability (Barba et al. 2021).  $\text{CH}_4$  emissions from trees in wetter soils may result from transport and diffusion across the soil-stem interface, evidenced by declining  $\text{CH}_4$  emissions with increasing stem height (van Haren et al. 2021).

Anatomical differences between functional and taxonomic groups, namely cell structure, aerenchyma presence, bark lenticel density, and resistance to wood rot, influence  $\text{CH}_4$  flux variability across tree species (Barba et al. 2019). Species with ring-porous wood structure and extensive aerenchyma tissue may exhibit greater gas diffusion and in turn higher  $\text{CH}_4$  emissions. However, individual trees of the same species under similar environmental conditions can exhibit dramatically different emissions (Terazawa et al. 2015). Stem diameter affects gas storage and diffusion, and tree age may have independent implications on microbial colonization, both of which may influence  $\text{CH}_4$  flux rates (Oberle et al. 2018; Moisan et al. 2024). Relating  $\text{CH}_4$  dynamics to  $\text{CO}_2$  flux (e.g., respiration) from tree stems could elucidate important predictors and underlying mechanisms for microbial generation of  $\text{CH}_4$  in soil-tree comparisons.  $\text{CO}_2$  and  $\text{CH}_4$  emissions may be positively related in some individuals, but not necessarily across all trees in an ecosystem (Pitz et al. 2018). Improving our understanding of functional relationships between  $\text{CH}_4$  flux,  $\text{CO}_2$  flux, and species- and individual-level traits would enhance predictive models for upscaling gas fluxes on an ecosystem level.

High local-scale spatial variability has been observed in tree stem  $\text{CH}_4$  emissions, even within the same tree species. Flux rates across transitional zones, such as upland-to-wetland gradients, remain poorly understood as well (Pitz et al. 2018). Projected increases in regional precipitation due to climate change threaten to shift net annual  $\text{CH}_4$  sinks into net  $\text{CH}_4$  sources (Fernandez et al. 2020), which could be exacerbated by stem emissions. Understanding temporal and spatial patterns of  $\text{CH}_4$  flux from forested

ecosystems may shed light on how flux rates and carbon budgets may be affected by climate change.

In this study, we measured  $\text{CH}_4$  and  $\text{CO}_2$  flux from living tree stems along an upland-to-wetland drainage gradient at the Howland Research Forest, which is a net annual sink of  $\text{CH}_4$ . Howland Forest is an upland conifer dominated forest in Maine, USA, that includes small forested wetlands, typical of the patchiness of this northern glaciated landscape. We randomly selected individual living *Picea rubens* (red spruce), *Tsuga canadensis* (eastern hemlock) and *Acer rubrum* (red maple) trees for  $\text{CH}_4$  flux measurements. Our overarching goal was to better understand tree  $\text{CH}_4$  fluxes in this northern conifer forest—an ecosystem that remains underrepresented in  $\text{CH}_4$  stem flux research. Our specific objectives include (1) identifying the environmental factors influencing tree stem  $\text{CH}_4$  flux, (2) characterizing differences in  $\text{CH}_4$  flux from three heights at the base of tree stems, and (3) assessing how tree stem  $\text{CH}_4$  flux varies spatially within this landscape, which includes upland-to-wetland gradients. Finally, we used results from these objectives to scale stem  $\text{CH}_4$  flux to the stand level.

## Methods

### Site description

This study was conducted at Howland Research Forest of central Maine, USA ( $45.2041^\circ\text{N}$   $68.7402^\circ\text{W}$ , elevation 60 m above sea level), located in the transition zone between deciduous and boreal forests in northeastern North America. The climate is damp and cool, with average annual temperatures of  $5.9 \pm 0.8^\circ\text{C}$  and mean precipitation of  $112 \pm 21\text{ cm}/\text{year}$  that is evenly distributed throughout the year (Daly et al. 2008). Mean daily temperature ranged from  $-1.2$  to  $26.6^\circ\text{C}$  with an average of  $15.2^\circ\text{C}$  from April to November, 2024. Daily precipitation ranged from 0 to  $41.3\text{ mm}$  with a sampling period mean of  $2.5\text{ mm}$ . Peak temperature occurred on August 2nd and peak precipitation occurred on August 9th.

The mature multi-aged forest is roughly 90% conifer, dominated by red spruce (*Picea rubens*, 51% of stand basal area) and eastern hemlock (*Tsuga canadensis*, 21%), with white pine (*Pinus strobus*) and northern white-cedar (*Thuja occidentalis*) present in lesser abundance. Hardwood presence is dominated

by red maple (*Acer rubrum*, 9% of stand basal area). The forest has remained unmanaged since a partial harvest in the 1920s and exhibits late-successional characteristics, such as large old trees ( $> 200$  years) and a range of tree diameters and coarse woody debris decay classes (Fien et al. 2019). The dominant soils were formed in coarse-loamy granitic basal till and range from well drained to poorly drained over relatively small areas along upland-wetland gradients (Fernandez et al. 1993).

### Data collection

We selected 51 living trees (27 red spruce, 15 eastern hemlock, 9 red maple) for  $\text{CH}_4$  flux sampling using a stratified random approach, with stratification based on species, tree diameter at breast height (DBH), and soil drainage class within a ca.  $400 \times 400\text{ m}$  area (Fig. 1a). Species and diameter data were obtained from 20 forest inventory plots ( $400\text{ m}^2$  each). Drainage classes (wetland, transitional, upland) were assigned based on soil moisture data obtained from 100 randomly placed sensors, as well as a National Wetlands Inventory wetland delineation. Soil moisture data were then used to produce a kriging-interpolated map (using ArcGIS Pro, version 3.2.4) of the landscape to approximate the area of each drainage class. Informed by these constraints, random points were generated within each drainage class, and a predetermined tree species-by-diameter combination was targeted for each point, ensuring a stratified distribution among drainage classes, species, and diameters. Finally, trees were selected in the field by identifying the closest tree within 10 m from each point that matched the species and diameter determination.

In order to measure  $\text{CH}_4$  flux from tree stem surfaces, we semi-permanently affixed circular collars to our selected trees. Collars were constructed from polyvinyl chloride pipe of 10 cm diameter with saddle-shaped faces of various sizes to fit to a range of tree diameters. Collars were then affixed to selected tree stems at a height of 50 cm using pure silicone (Fig. 1b). All collars were leak tested prior to each measurement by blowing on and around the collar, and additional silicone was applied as needed. To assess the transport and generation of  $\text{CH}_4$  emissions along the tree stem (Wang et al. 2016; Martinez et al. 2022) additional chambers were installed on a

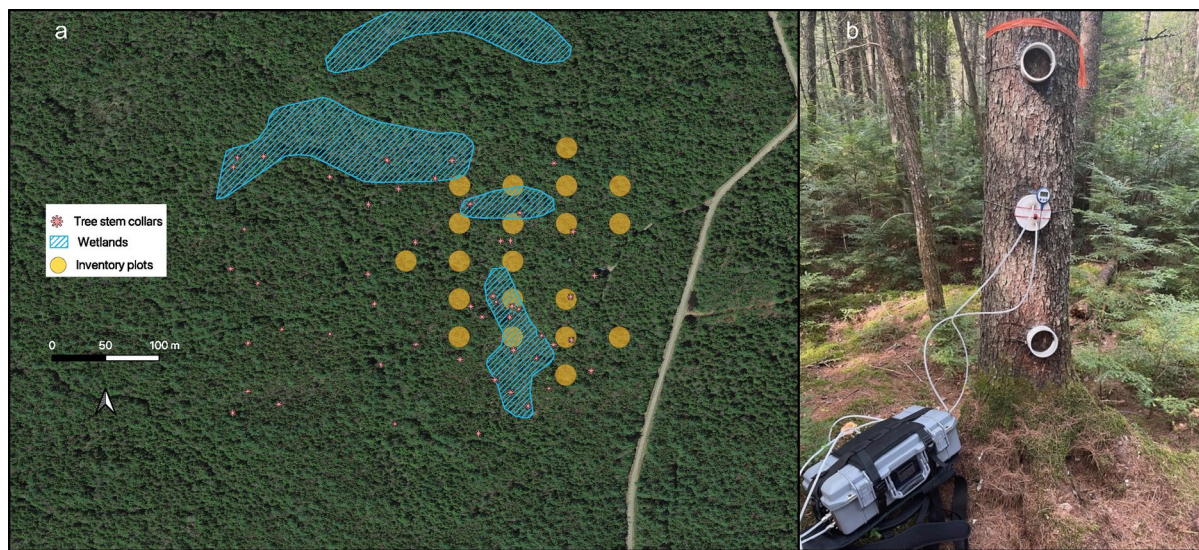


**Fig. 1** **a** Sampling collars for  $\text{CH}_4$  measurements, inventory plots ( $400 \text{ m}^2$ ) and designated wetlands. **b** Red spruce tree stem with chambers at 50 cm, 100 cm, and 150 cm above the forest floor, with chamber cap and IRGA attached for flux sampling

subset ( $n=10$ ) of spruce trees at 100 cm and 150 cm heights. We refer to these as 'height trees.'

$\text{CH}_4$  and  $\text{CO}_2$  concentrations were measured by sealing each collar with a custom PVC chamber cap connected via 3 m of 6.4 mm ( $\frac{1}{4}$ -inch) diameter Bev-A-Line tubing to a LI-COR LI-7810, as described in Read et al. (2023). After flushing with ambient air (ca. 2000 ppb  $\text{CH}_4$ ) until a stable baseline for gas concentration was achieved, manual fluxes were measured at 1 Hz over six-minute intervals per flux observation and processed as described below, alongside instantaneous measurements of air temperature, soil temperature, and soil moisture (volumetric water content, %VWC) (see below). Flux measurements, including all collars across species and heights, were collected every two weeks, from late-April, following snowmelt, until mid-November 2024, yielding a total of 750 measurements.

We collected a set of environmental variables to be tested as potential predictors of  $\text{CH}_4$  flux rates. Instantaneous air temperature was collected with a Traceable Precision Lollipop Digital Thermometer; soil moisture and temperature were measured at three points around the tree with an Acclima True TDR-315N Soil Moisture Sensor (15 cm depth). Soil pH was determined at the base of each tree by collecting full depth of organic layer on 18 July (five days after a rain event) and electrometrically measuring pH of

dried soil suspended in deionized water (1:2 ratio) (Gavlak 2005). Hemispherical photographs were taken at three points around each tree (two meters from stem, at bearings 0, 120 and 240°) using a Nikon Coolpix 995 camera with a hemispherical lens adapter. Photographs were processed using Gap Light Analyzer software (Frazer et al. 1999) to yield canopy openness values.

#### Data processing

Fluxes for  $\text{CH}_4$  ( $\text{nmol m}^{-2} \text{ s}^{-1}$ ) and  $\text{CO}_2$  ( $\mu\text{mol m}^{-2} \text{ s}^{-1}$ ) were calculated from the gas analyzer output files using the ideal gas law, where  $PV = nRT$  ( $P$  = barometric pressure, atm,  $V$  = chamber volume, L (liters),  $R$  (gas constant) = 0.08206 L·atm/mol·K,  $T$  = temperature, °C):

$$\text{Flux} = \left( \frac{dC}{dt} \right) \left( \frac{V}{A} \right) \frac{P}{(R * (T + 273.15))}$$

The change in gas concentration over time ( $dC/dt$ ) was calculated from 90 to 345 s for each sampling based on gas analyzer data outputs of gas concentration vs. time. This time window was selected to minimize chamber sealing effects and initial concentration spikes observed from wetland trees. Barometric pressure ( $P$ ) was matched with the closest 30-min-interval

measurement from an on-site pressure sensor. Chamber volumes (V) were determined in the laboratory for each chamber size by placing a curve-fitting seal over the tree-facing side of the chamber, filling with quinoa seeds (or any granular substance), and measuring the volume of those seeds. Areas (A) of tree stem surface were also determined for each size template. Air temperature (C°) at the time of sampling was converted to Kelvins (K) prior to flux calculations. Minimum detectable flux was estimated for each measurement according to Christiansen et al. (2015) and Nickerson (2016); all fluxes were within the detection limit. All data processing and statistics were conducted in R (R Core Team 2024) using RStudio (Posit Team 2024).

### Data analysis

In order to identify the predictors most strongly influencing our response variable, tree CH<sub>4</sub> flux, we used three analytical approaches. First, we used a linear mixed-effects model with tree species and environmental drivers as fixed effects. Results revealed significant interaction effects between species, soil moisture, and soil temperature, justifying the use of species-specific models. Second, to further evaluate how fluxes differed by species, we conducted a two-way ANOVA with tree species and drainage class as the main effects. We binned this analysis by drainage class because eastern hemlock did not occur in the wetlands. Lastly, to assess species-specific environmental drivers of stem CH<sub>4</sub> flux, we developed linear mixed-effects models for each tree species. Soil moisture (continuous), soil temperature, air temperature, soil pH, canopy openness, elevation, stem diameter, and CO<sub>2</sub> flux rates were selected as potential predictor variables. Our approach to developing these species-specific linear models is described as follows.

Random forest analysis of the potential predictors, which was done using the *Boruta* package in R (Kursa and Rudnicki 2010), deemed soil pH as not important and all other variables as important. For each species, linear mixed-effects models were analyzed using the “lmer” function in the *lme4* package in R (Pinheiro 2021). We tested various combinations of important predictors, both interactive and additive, using a deductive approach of omitting variables that were not statistically significant based on p-values. We then compared models based on corrected Akaike’s

information criterion (AICc), allowing us to assess which model forms were best supported by the data. The interaction between soil moisture and soil temperature was the only significant interaction included in the top models, as all other tested interactions between predictor variables were not statistically significant. Day of year and tree identifier (i.e. individual tree sample) were included as random variables to account for within-day and between-tree variation in flux. CH<sub>4</sub> flux was natural-log transformed prior to analyses to ensure normality of model residuals. All predictor variables were standardized (mean=0, standard deviation=1) before model fitting to allow us to compare effect sizes among predictors having different units. Elevation and canopy openness were omitted from models because they were colinear with soil moisture (variance inflation factor>5); soil moisture was retained because, unlike these isolated variables, it captures both within-day fluctuations and seasonal variability.

Visual assessment of CH<sub>4</sub> flux vs. soil moisture graphs for spruce and maple suggested moisture thresholds beyond which flux markedly increased. We tested for the presence of these thresholds, or breakpoints, for each species using segmented regressions, where natural-log transformed CH<sub>4</sub> flux was the response variable and soil moisture the predictor variable. To isolate the effect of soil moisture, soil temperature was held constant in linear models used to generate breakpoint analyses. We accomplished this by modeling flux as a response to the interaction between soil moisture and temperature, then generating a predicted flux based on the mean soil temperature over the sampling period. Analyses were conducted using the *segmented* package in R (Fasola et al. 2018).

To assess differences in CH<sub>4</sub> flux along the red spruce stem height profile, we binned the fluxes from our 10 height trees by drainage class and performed three one-way ANOVAs followed by Tukey’s tests. This approach allowed us to compare fluxes between the three heights within each drainage class, providing insights into CH<sub>4</sub> transport from stems along an upland-to-wetland drainage gradient.

To assess how tree CH<sub>4</sub> flux (as well as selected predictor variables) varied spatially within this small landscape, we used the large number of geo-referenced fluxes and soil moisture and temperature readings (collected from 80 points throughout sampling period),

in addition to our hemispherical photographs ( $N=90$  from trees and plot locations). We first tested for spatial autocorrelation of these individual variables using semivariogram functions (lag size=59 and number of lags=12), followed by Gaussian model inference to produce kriged surfaces of stem flux, soil moisture, soil temperature, and canopy openness, using ArcGIS Pro (version 3.2.4) (Esri 2024). Comparative analysis of the interpolated data, which included sampling-period averaged flux and environmental drivers, was conducted with a simple Pearson correlation.

### Scaling

Finally, we scaled  $\text{CH}_4$  flux from tree stem chamber areas to individual tree  $\text{CH}_4$  flux (up to 150 cm height) using stem surface area ( $\text{m}^2$ ) estimations. For all sampled trees, stem surface area was calculated based on field measured diameters taken at 150 cm height and at tree base, assuming the shape of conical frusta ( $R=\text{radius at } 150 \text{ cm height}$ ,  $r=\text{radius at tree base}$ ,  $l=150 \text{ cm}$ )

$$\text{Stem Surface Area} = \pi(R + r) \cdot l$$

This approach allowed us to develop a relationship between stem surface area and diameter (breast height), the latter of which was measured for all inventoried trees, and thus predict stem surface area for all

inventoried trees. We then calculated species-specific stem flux averages for each month (April–November). Stem fluxes along the height gradient were modeled as a negative exponential function using our height tree dataset, grouping trees by drainage class to account for the influence of soil moisture on  $\text{CH}_4$  flux at different heights. These individual stem fluxes were then scaled to the plot-level using data from twenty 400  $\text{m}^2$  inventory plots. Assuming our sampling and inventory schemes were representative of the landscape, and that no diel patterns in flux existed, we then used Monte Carlo simulation to estimate total  $\text{CH}_4$  emission ( $\text{mmol ha}^{-1} \text{h}^{-1}$ ), for each tree species, from lower tree stems. We performed 1,000 simulations, each randomly selecting 10 plots from our dataset to account for variability in environmental conditions and flux rates across individuals. This approach provided a robust estimate of stand-level, lower stem  $\text{CH}_4$  flux while incorporating uncertainty in spatial heterogeneity.

### Results

Sampling period tree stem  $\text{CH}_4$  fluxes ranged from -0.03 to 31.58  $\text{nmol m}^{-2} \text{s}^{-1}$  and were highest from mid-July to mid-August (Fig. 2a).  $\text{CH}_4$  uptake was observed only seven times out of 730 measurements throughout the sampling period, all of which

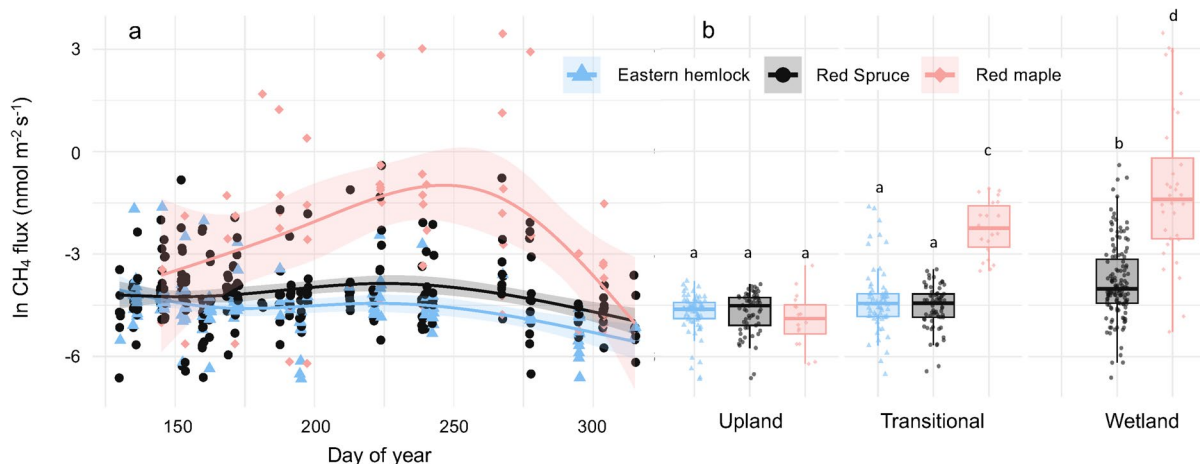


**Fig. 2** **a** Relationship between  $\text{CH}_4$  flux ( $\text{nmol m}^{-2} \text{s}^{-1}$ ) and day of year across three tree species. The shaded regions around each spline represent the 95% confidence interval, calculated using standard errors from the smoothing model. **(b)**

$\text{CH}_4$  fluxes binned by drainage class and species. Statistical differences indicated by lowercase letters. Note that hemlocks did not occur in the wetland areas and negative fluxes ( $n=7$ ) were omitted because of the log-scale

occurred on upland trees, at 50 cm stem height, during the shoulder seasons (Spring and Fall). Mean flux approached zero between October (275th day of year) and November, with an average flux rate of  $0.005 \text{ nmol m}^{-2} \text{ s}^{-1}$  in November. Mean fluxes also varied by tree species (red maple highest) and soil drainage class (wetlands highest) (Fig. 2b).

Stem fluxes were highest overall in the wetlands when compared to transitional or upland fluxes ( $p$  values  $<0.008$ ); however, transitional and upland fluxes did not differ from each other ( $p=0.666$ ). The wetland gradient also appeared to accentuate tree species differences. Within the upland soils, fluxes did not differ among species ( $p=0.332$ ); however, red maple fluxes were significantly greater than those of spruce and hemlock in both transitional and wetland (both  $p<0.001$ ) soils. Red spruce fluxes did not differ from those of eastern hemlock in upland and transitional soils.

Linear mixed-effects models showed a strong positive relationship between stem  $\text{CH}_4$  emissions and soil moisture. For all species, soil moisture was the most important predictor and was included in the top models (i.e., lowest AIC scores). Models also revealed species-specific relationships between  $\text{CH}_4$  flux and predictor variables, as quantified by

standardized effect sizes (Fig. 3). Fluxes from eastern hemlock stems were best explained by positive effects of soil moisture and tree diameter. For red spruce, the top model included a positive interaction between soil moisture and soil temperature, with additional variability explained by air temperature.  $\text{CH}_4$  flux from red maple similarly showed a positive response to the interaction between soil moisture and soil temperature in the top model, with stem diameter explaining some variability in other top-performing models (Table 1). The interaction between soil moisture and soil temperature in  $\text{CH}_4$  fluxes from red spruce and red maple indicates that flux rates depend on both factors, with simultaneous increases amplifying the effect (Fig. 4).

The segmented regression analysis further emphasized the positive relationship between soil moisture and  $\text{CH}_4$  flux. Results revealed thresholds in soil moisture above which  $\text{CH}_4$  flux rates increased dramatically, when soil temperature was held constant at  $14^\circ\text{C}$  (Fig. 5). The breakpoints were similar for red spruce and red maple at  $\sim 60\%$  soil moisture. We conducted a segmented regression for eastern hemlock, but no breakpoint was identified, given the limited range of moisture conditions under which it occurred.

**Fig. 3** Effect sizes from top linear mixed-effects models for each species. Variables were selected based on  $p$  values, AIC scores, and residual distributions. Significance levels are also shown ( $*=0.1$ ,  $**=0.05$ ,  $***=0.01$ ,  $****=0.001$ )

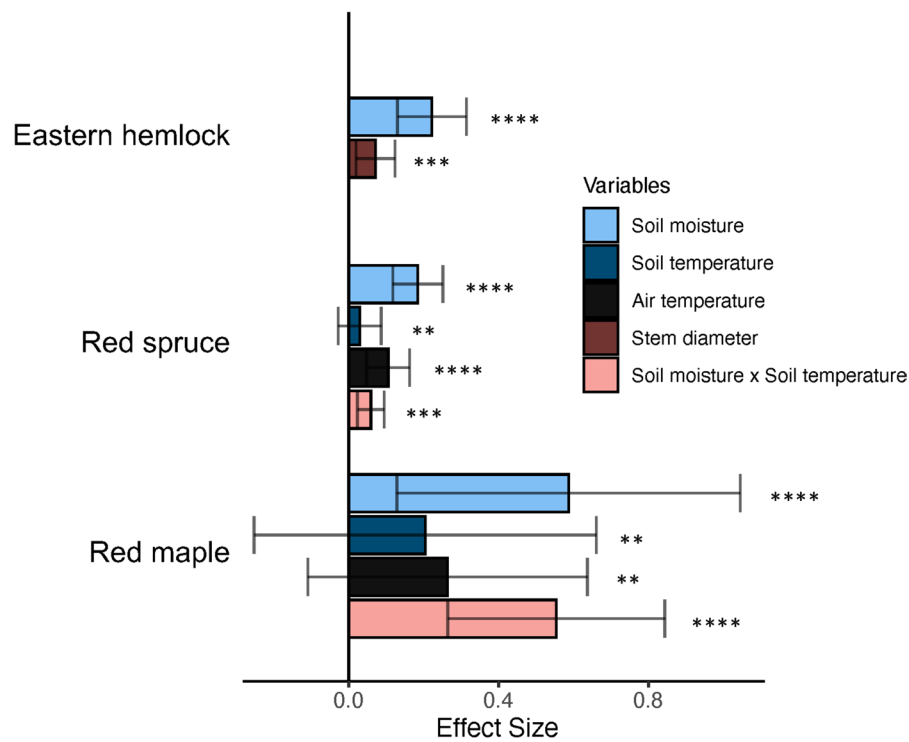


**Table 1** Top three models for each species, ranked by increasing AICc scores, where  $k$  represents the number of estimated parameters,  $cR^2$  represents the conditional  $R^2$ ,  $mR^2$  represents the marginal  $R^2$

Species	Model predictors	$k$	AICc	$\Delta$ AICc	AICc wt	$cR^2$	$mR^2$
Eastern hemlock	Soil mois. + Stem diam	6	18.2	0.0	0.6	0.55	0.25
	Soil mois	5	19.8	1.6	0.3	0.54	0.17
	Soil mois. + Soil temp. + Air temp. + Stem diam	8	22.5	4.3	0.1	0.49	0.33
Red spruce	Soil mois. x Soil temp. + Air temp	8	268.1	0.0	0.7	0.56	0.33
	Soil mois. + Air temp	6	270.1	2.0	0.2	0.54	0.31
	Soil mois. x Stem diam. + Air temp	8	270.6	2.5	0.1	0.52	0.28
Red maple	Soil mois. x Soil temp. + Air temp	8	225.9	0.0	0.8	0.74	0.59
	Soil mois. x Soil temp. x Stem diam	9	229.2	3.3	0.1	0.73	0.59
	Soil mois. x Soil temp. + Stem diam. + Air temp	11	232.4	6.5	0.1	0.74	0.65

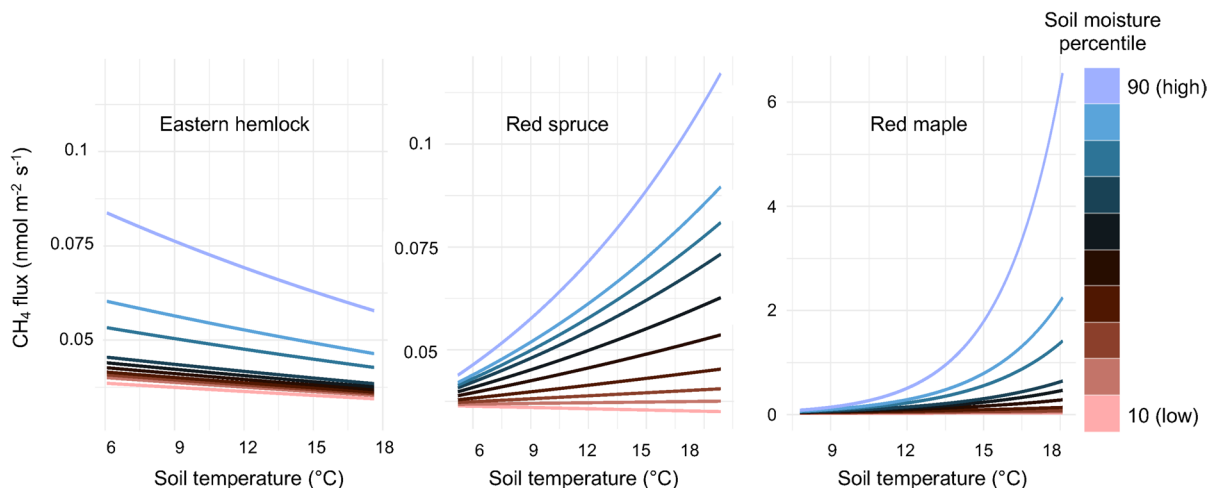


**Fig. 4** Response of  $\text{CH}_4$  flux to soil temperature from low to high soil moisture percentiles, emphasizing the interaction between soil moisture and soil temperature for red spruce and red maple

For red spruce trees in the wetlands, we found that  $\text{CH}_4$  stem flux decreased significantly with increasing stem height ( $p=0.035$ ) when tested at 50, 100, and 150 cm (Fig. 6). In contrast, red spruce trees in the transitional or upland soils showed no differences in flux rates along the height profile ( $p$  values  $>0.656$ ).

Pearson's correlation tests showed strong correlation ( $r=0.72$ ) between stem  $\text{CH}_4$  flux and soil moisture based on kriging-interpolated point datasets (Fig. 7). Flux was only weakly correlated with soil temperature ( $r=0.28$ ) and canopy openness ( $r=0.21$ ).

Once scaled to a per-hectare basis and averaged across drainage classes, our estimates for peak-season (July and August) tree stem flux (up to 150 cm height on stem) at this site are the

following:  $10 \pm 3 \text{ } \mu\text{mol ha}^{-1} \text{ h}^{-1}$  for eastern hemlock,  $42 \pm 8 \text{ } \mu\text{mol ha}^{-1} \text{ h}^{-1}$  for red spruce, and  $120 \pm 41 \text{ } \mu\text{mol ha}^{-1} \text{ h}^{-1}$  for red maple. Our estimates for tree stem (up to 150 cm height)  $\text{CH}_4$  emissions integrated from April to November at Howland Research Forest are the following:  $1 \pm 0.2 \text{ kg CH}_4/\text{ha}$  for eastern hemlock,  $3 \pm 0.5 \text{ kg CH}_4/\text{ha}$  for red spruce, and  $8 \pm 4.1 \text{ kg CH}_4/\text{ha}$  for red maple.

## Discussion

Results from this study highlight the magnitude and direction of tree stem  $\text{CH}_4$  fluxes, revealing seasonal trends and key biophysical drivers that shape

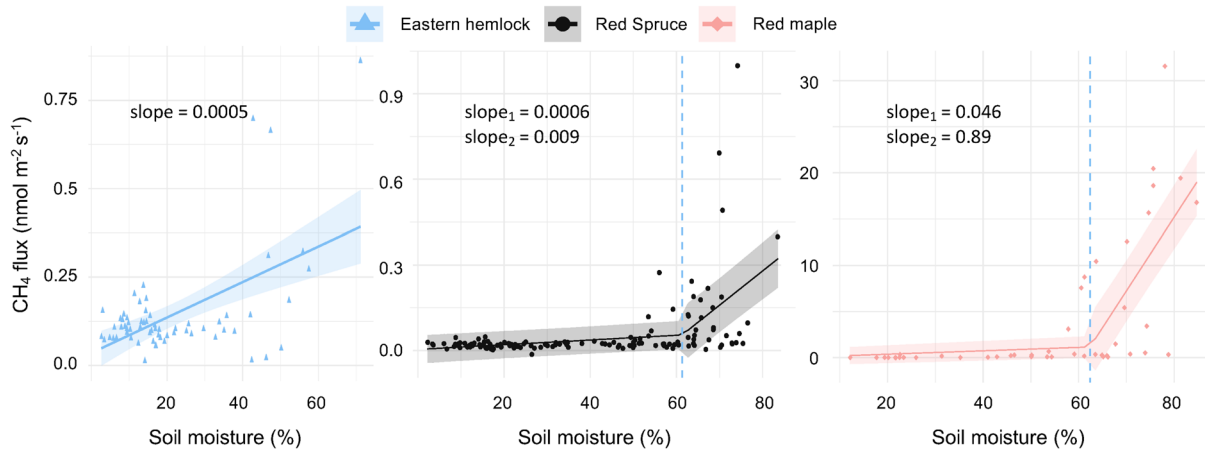


**Fig. 5** Segmented linear regressions for red spruce and red maple at constant soil temperature. Shaded areas around lines represent 95% confidence intervals and dashed vertical lines represent soil moisture breakpoints (61% for red spruce and

62% for red maple), beyond which  $\text{CH}_4$  flux increased markedly. Regression slopes before ( $\text{slope}_1$ ) and after ( $\text{slope}_2$ ) breakpoints are shown as well

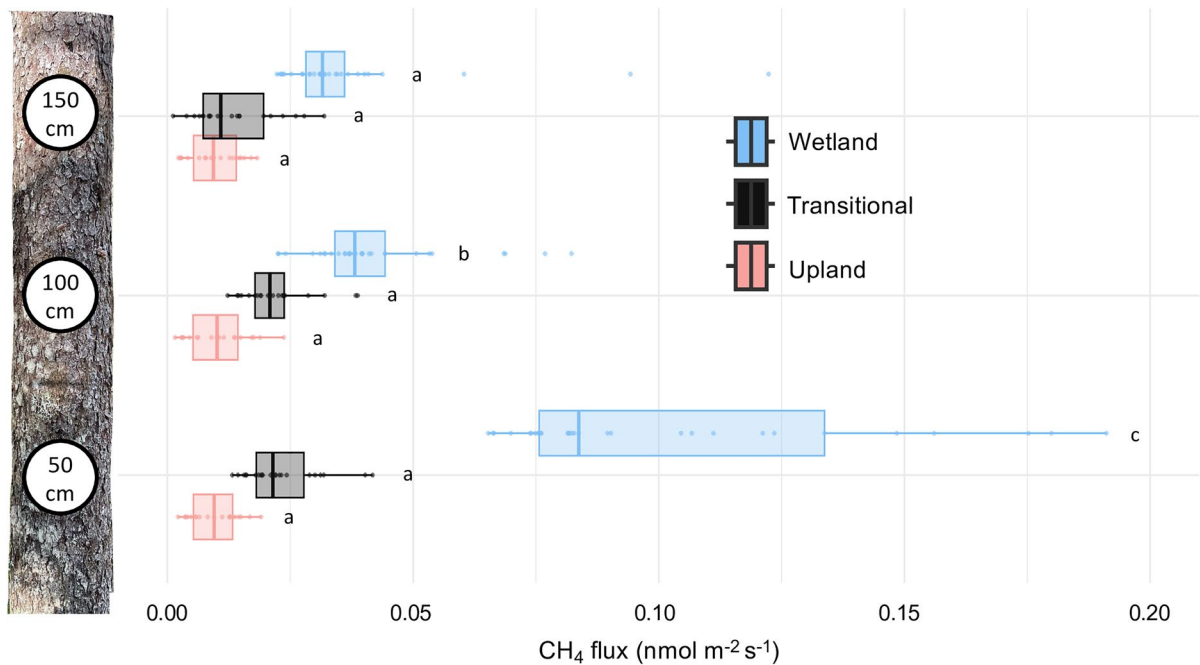


**Fig. 6**  $\text{CH}_4$  flux rates (x-axis) at 50, 100, and 150 cm stem height (y-axis) for upland, transitional, and wetland red spruce height trees. Boxes represent interquartile ranges, and whiskers

extend to minimum and maximum values. Letters indicate significant differences among heights within a drainage class

their variability. We observed higher emissions in wetter soils and during the warmest weeks of the sampling period, with high variability within and among species. While we did at times find minimal

$\text{CH}_4$  uptake ( $n=7$  observations), emission was the dominant observation ( $n=723$ ) across all drainage classes, species, and sampling heights.

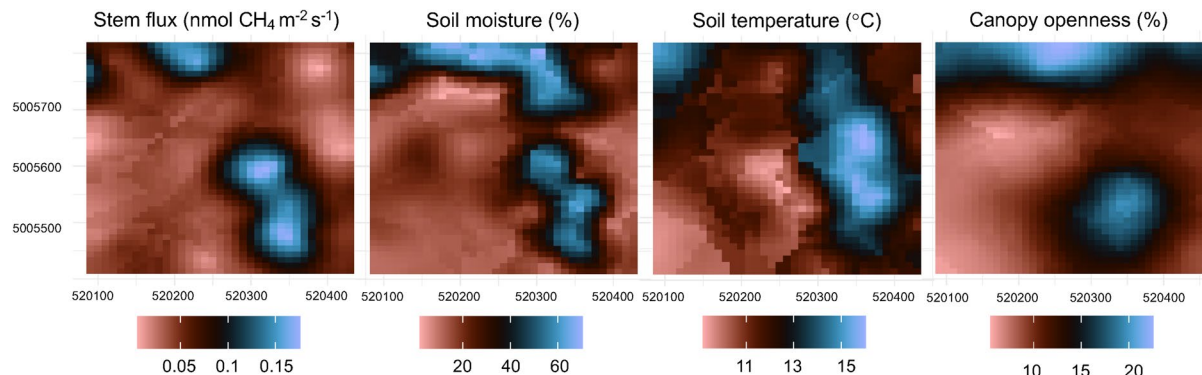


**Fig. 7** Kriging interpolated maps of  $\text{CH}_4$  stem flux, soil moisture, soil temperature, and canopy openness, where higher values are expressed as blue and lower values as red. Kriged area

is roughly  $400 \times 400$  m. Longitude and latitude coordinates (UTM Zone 19) are shown on the axes

### Stem $\text{CH}_4$ emissions increase along upland-to-wetland gradient

Our results demonstrated an increase in tree stem  $\text{CH}_4$  flux along the drainage gradient from upland to wetland. Soil moisture was the most important single predictor for all species. Similarly, previous studies have demonstrated a positive relationship between tree stem  $\text{CH}_4$  flux and soil moisture (Sjögersten et al. 2020; Feng et al. 2022). Our models further suggest that for red maple and red spruce, soil moisture and soil temperature interact to positively influence  $\text{CH}_4$  flux. That is, at high soil moisture,  $\text{CH}_4$  flux response to increasing temperature was more positive. This finding may be explained by temperature sensitivity of both methanogenesis and plant-mediated transport in high soil moisture conditions. While methanogens are typically more abundant in soils, recent research suggests that methanogens can also inhabit tree stems, particularly in wetter environments, and contribute to increased  $\text{CH}_4$  emissions from stems (Yip et al. 2019; Harada et al. 2024).

Wetland trees at this site were smaller, which may have confounded the diameter effect. In fact, hemlock lacked the soil moisture  $\times$  soil temperature interaction observed in the other species, possibly because it did not occur in wetlands and thus lacked the full range of soil moisture. This constraint could explain the positive effect of stem diameter on  $\text{CH}_4$  emissions in hemlock: without the presence of wetland trees, which are typically smaller in diameter, hemlock was the only species for which stem

diameter had a significant and positive influence on  $\text{CH}_4$  flux. Note also that these fluxes are expressed per unit area, but surface area scales exponentially with diameter. Therefore, the total flux from the tree also scales exponentially with diameter, even when emissions per unit surface area remain constant. This result is in contrast with previous studies, which have identified a negative relationship between  $\text{CH}_4$  flux (per unit surface area) and stem diameter in both upland (Klaus et al. 2024) and wetland (Pangala et al. 2013) tree stems.

Importantly, for red maple and red spruce, we identified a “breakpoint” in soil moisture ( $\sim 60\%$  VWC) beyond which  $\text{CH}_4$  flux rates increased significantly. This breakpoint is in strong agreement with previously reported soil moisture values (Koschorreck and Conrad 1993; Castro et al. 1995; Bowden et al. 1998). We did not identify a breakpoint for eastern hemlock; as above, this species did not occur in the wetlands. The breakpoint has important implications in light of projected increases in precipitation for this region (Fernandez et al. 2020). Given these expected changes in regional climate, Howland Forest could transition from a net annual  $\text{CH}_4$  sink to source, with tree stems serving as a major conduit for methanogenesis in wetland areas (Shoemaker et al. 2014). Assuming plant-mediated transport of  $\text{CH}_4$  from soils, this breakpoint provides further circumstantial evidence for soil transition from net methanotrophy to net methanogenesis (von Fischer and Hedin 2007), and may indicate a threshold below which tree-emitted  $\text{CH}_4$  is primarily produced within stem tissue, and

above which soil-derived  $\text{CH}_4$  is additionally transported and emitted.

#### Stem $\text{CH}_4$ flux varies by species

Our results indicate significant species-level differences in  $\text{CH}_4$  flux from tree stems. We found higher  $\text{CH}_4$  emissions from red maples compared to the conifers, particularly in wetter soils. Higher  $\text{CH}_4$  emissions from hardwood species compared to softwoods has been observed in a boreal ecosystem across a similar moisture gradient (Vainio et al. 2022). We also observed a more rapid flux increase beyond the upland-wetland breakpoint for red maple than for red spruce. Combined, these results suggest a stronger and more consistent positive response of red maple  $\text{CH}_4$  fluxes to soil moisture, which may reflect potential species-specific physiological or microbial interactions that affect  $\text{CH}_4$  transport, methanogenesis, and methanotrophy (Moisan et al. 2024). Previous studies have noted species-level trait differences in  $\text{CH}_4$  emissions from tree stems, which may further be attributed to factors such as wood density, bark structure, root distribution, aerenchyma presence, and/or lenticel density (Pangala et al. 2013; Pitz et al. 2018).

We also found high within-species variability in  $\text{CH}_4$  flux, with red maple showing the highest variability, particularly in transitional and wetland soils. Our linear models, consisting of biophysical variables, explain only a portion of this variability (25 to 65% depending on species, based on marginal  $R^2$  values). Therefore, individual-level traits of trees or their underlying soils likely influence differences in  $\text{CH}_4$  flux rates that cannot be explained by species traits or environmental conditions alone (Barba et al. 2021). While tree diameter did not influence flux rates across species in our study, tree age, root structure, and aerenchyma tissue have been identified as potential predictors for explaining variability among individuals (Barba et al. 2019). In the wetland areas, the high spatial variability of  $\text{CH}_4$  flux from wetland soils may help to explain variance in stem-transported  $\text{CH}_4$  emissions (Jeffrey et al. 2023). Meanwhile, in the upland areas, variance in methanogenesis may be more strongly associated with tree tissue internal anoxia, wetwood, and/or decay, all of which are highly variable among individuals (Hietala et al. 2015; Covey and Megonigal 2019).

$\text{CH}_4$  fluxes from lower stems are predominantly emissions

While our  $\text{CH}_4$  stem measurements were overwhelmingly net emissions, this does not discount the possibility of gross uptake (i.e., methanotrophy) on any tree surface, nor of net uptake at higher stem heights, especially considering that our upland stem net emissions were very low (mean  $0.012 \pm 0.009 \text{ nmol m}^{-2} \text{ s}^{-1}$ ) and that measurements were limited to low tree heights ( $< 2 \text{ m}$ ). Methanotrophic bacteria have been identified in bark, sapwood, and heartwood of living tree stems (Jeffrey et al. 2021; Feng et al. 2022; Arnold et al. 2024), and net  $\text{CH}_4$  uptake has been directly measured from tree stems (Gauci et al. 2024). The balance between methanotrophy and methanogenesis in tree stems likely depends on a complex interplay among microbial communities, oxygen availability, and substrate supply, which may vary across species and environmental conditions (Pitz and Megonigal 2017; Barba et al. 2024). Seasonal shifts in temperature, precipitation, and soil moisture could further influence these processes, potentially leading to periods of net uptake or enhanced emissions. Additionally, biophysical factors such as tree age, stem diameter, and wood porosity may shape the balance between  $\text{CH}_4$  emissions and uptake.

#### $\text{CH}_4$ flux varies by stem height in wetlands

We found decreasing  $\text{CH}_4$  fluxes with increasing stem height for wetland trees and observed no such trend for upland and transitional trees. Tree stems may represent a major pathway for forested wetland  $\text{CH}_4$  emissions, largely through gas transport, sap flow, and diffusion from soil methanogenesis (Covey and Megonigal 2019). As above, many studies have shown that  $\text{CH}_4$  can also be produced via methanogenesis within trees (Pangala et al. 2013; Jeffrey et al. 2023). However, our results suggest that soil methanogenesis likely dominates the relatively high  $\text{CH}_4$  efflux from wetland trees in this system. Meanwhile, the balance of uptake and emissions, from both soil and tree-hosted methanogenesis and methanotrophy, may be more complex. Future studies of  $\text{CH}_4$  flux from tree stems could benefit by sampling at more heights along the stem and further exploring zones

of gross production and gross uptake throughout the plant-soil system.

#### CH<sub>4</sub> flux correlates spatially with soil moisture

Spatial analysis provided insights into landscape-level hotspots and drivers of CH<sub>4</sub> flux from tree stems. Both a visual interpretation of the kriged images and statistical results point to soil moisture as a major control on stem CH<sub>4</sub> flux, potentially influencing microbial activity and CH<sub>4</sub> transport processes across the soil-tree interface. In contrast, the weak correlation with soil temperature indicates that temperature-driven metabolic processes or within-growing-season variations may play a lesser role in governing stem CH<sub>4</sub> flux at this site (Vainio et al. 2022). Similarly, the weak correlation with canopy openness suggests that light availability and associated vegetation structure have minimal direct influence, possibly because stem-mediated CH<sub>4</sub> flux is more strongly tied to below-ground hydrological and microbial dynamics or conditions within the tree stem. These findings highlight the importance of subsurface moisture conditions in shaping tree-stem CH<sub>4</sub> emissions and emphasize the need for further investigation into the mechanisms linking soil hydrology with stem gas exchange.

## Conclusion

Our study demonstrates that tree stems in this northern conifer forest predominantly emitted CH<sub>4</sub>, with emissions highest during mid-summer and in wetland areas. Soil moisture emerged as the strongest predictor of stem CH<sub>4</sub> flux across all studied species, with a critical threshold (~60% VWC) identified beyond which emissions increased dramatically for red maple and red spruce. Major species differences were evident, with red maple stems emitting significantly more CH<sub>4</sub> than conifer species (peak-season estimates:  $10 \pm 3 \text{ } \mu\text{mol ha}^{-1} \text{ h}^{-1}$  for eastern hemlock,  $42 \pm 8 \text{ } \mu\text{mol ha}^{-1} \text{ h}^{-1}$  for red spruce, and  $120 \pm 41 \text{ } \mu\text{mol ha}^{-1} \text{ h}^{-1}$  for red maple). These species differences were most pronounced in wetter landscape positions.

Temperature response depended on moisture, with soil moisture and soil temperature interacting to influence CH<sub>4</sub> flux in red maple and red spruce. Circumstantial evidence for soil origin of wetland

tree emissions was observed through height profiles and moisture breakpoints, with wetland tree stems showing decreasing CH<sub>4</sub> flux with increasing stem height. Substantial intraspecific variation in CH<sub>4</sub> flux remained unexplained by environmental factors, suggesting individual-level traits or condition may significantly influence differences beyond species and environmental controls. Spatial analysis confirmed soil moisture as the primary control on stem CH<sub>4</sub> flux across the landscape. As climate change drives increases in precipitation across northeastern North America, these findings suggest that forests could transition from CH<sub>4</sub> sinks to sources, with tree stems—particularly of hardwood species like red maple—serving as increasingly important pathways in the global CH<sub>4</sub> cycle.

Taken together, our results highlight the need for additional work addressing stem CH<sub>4</sub> fluxes higher on the stem and canopy. Specifically, the biophysical and physiological controls on the balance between emissions and uptake are poorly understood. Additionally, more work on the soil-stem-foliar interface of CH<sub>4</sub> flux would improve our understanding of the relative contribution of trees to the net ecosystem CH<sub>4</sub> flux, which is required to characterize their role in global biogeochemical cycling.

**Author contributions** All authors contributed to the study conception and design. Material preparation, data collection and analysis were performed by CH. The first draft of the manuscript was written by CH and all authors commented on previous versions of the manuscript. All authors read and approved the final manuscript.

**Funding** This research was supported in part by the U.S. National Science Foundation (DEB Award #2208658, 2208655), the U.S. Department of Energy's Office of Science (AmeriFlux core site), the U.S. Forest Service, Northern Research Station (JVA #25-JV-11242306-009), Maine Agricultural and Forest Experiment Station (ME042612, ME042121), and NSF Graduate Research Fellowship to J.G.

**Data availability** The datasets generated and analyzed during this study have been made available in the Environmental Data Initiative (EDI) repository, accessible here: (<https://doi.org/10.6073/pasta/03586624214245c96a0399509ab4e3cb>).

## Declarations

**Conflict of interest** The authors have no relevant financial or non-financial interests to disclose.

**Open Access** This article is licensed under a Creative Commons Attribution-NonCommercial-NoDerivatives 4.0

International License, which permits any non-commercial use, sharing, distribution and reproduction in any medium or format, as long as you give appropriate credit to the original author(s) and the source, provide a link to the Creative Commons licence, and indicate if you modified the licensed material. You do not have permission under this licence to share adapted material derived from this article or parts of it. The images or other third party material in this article are included in the article's Creative Commons licence, unless indicated otherwise in a credit line to the material. If material is not included in the article's Creative Commons licence and your intended use is not permitted by statutory regulation or exceeds the permitted use, you will need to obtain permission directly from the copyright holder. To view a copy of this licence, visit <http://creativecommons.org/licenses/by-nc-nd/4.0/>.

## References

Arnold W, Gewirtzman J, Raymond PA, Bradford MA, Butler C, Peccia J (2024) A method for sampling the living wood microbiome. *Methods Ecol Evol* 15:1084–1096. <https://doi.org/10.1111/2041-210X.14311>

Barba J, Bradford MA, Brewer PE, Bruhn D, Covey K, van Haren J, Megonigal JP, Mikkelsen TN, Pangala SR, Pihlatie M, Poulter B, Rivas-Ubach A, Schadt CW, Terazawa K, Warner DL, Zhang Z, Vargas R (2019) Methane emissions from tree stems: a new frontier in the global carbon cycle. *New Phytol* 222:18–28. <https://doi.org/10.1111/nph.15582>

Barba J, Poyatos R, Capooci M, Vargas R (2021) Spatiotemporal variability and origin of CO<sub>2</sub> and CH<sub>4</sub> tree stem fluxes in an upland forest. *Glob Chang Biol* 27:4879–4893

Barba J, Brewer PE, Pangala SR, Machacova K (2024) Methane emissions from tree stems – current knowledge and challenges: an introduction to a virtual issue. *New Phytol* 241:1377–1380. <https://doi.org/10.1111/nph.19512>

Bowden RD, Newkirk KM, Rullo GM (1998) Carbon dioxide and methane fluxes by a forest soil under laboratory-controlled moisture and temperature conditions. *Soil Biol Biochem* 30:1591–1597. [https://doi.org/10.1016/S0038-0717\(97\)00228-9](https://doi.org/10.1016/S0038-0717(97)00228-9)

Castro MS, Steudler PA, Melillo JM, Aber JD, Bowden RD (1995) Factors controlling atmospheric methane consumption by temperate forest soils. *Glob Biogeochem Cycles* 9:1–10. <https://doi.org/10.1029/94GB02651>

Christiansen J, Outhwaite J, Smukler S (2015) Comparison of CO<sub>2</sub>, CH<sub>4</sub> and N<sub>2</sub>O soil-atmosphere exchange measured in static chambers with cavity ring-down spectroscopy and gas chromatography. *Agric for Meteorol* 211:48–47. <https://doi.org/10.1016/j.agrformet.2015.06.004>

Covey KR, Megonigal JP (2019) Methane production and emissions in trees and forests. *New Phytol* 222:35–51. <https://doi.org/10.1111/nph.15624>

Daly C, Halbleib MD, Smith JI, Gibson W, Doggett MK, Taylor GH, Curtis JM, Pasteris PP (2008) Physiographically sensitive mapping of climatological temperature and precipitation across the conterminous United States. *Int J Climatol* 28:2031–2064. <https://doi.org/10.1002/joc.1688>

Esri (2024) ArcGIS Pro

Fasola S, Muggeo VMR, Küchenhoff H (2018) A heuristic, iterative algorithm for change-point detection in abrupt change models. *Comput Stat* 33:997–1015. <https://doi.org/10.1007/s00180-017-0740-4>

Feng H, Guo J, Ma X, Han M, Kneeshaw D, Sun H, Malghani S, Chen H, Wang W (2022) Methane emissions may be driven by hydrogenotrophic methanogens inhabiting the stem tissues of poplar. *New Phytol* 233:182–193. <https://doi.org/10.1111/nph.17778>

Fernandez IJ, Son Y, Kraske CR, Rustad LE, David MB (1993) Soil carbon dioxide characteristics under different forest types and after harvest. *Soil Sci Soc Am J* 57:1115–1121. <https://doi.org/10.2136/sssaj1993.03615995005700040039x>

Fernandez IJ, Birkel S, Schmitt C V, Simonson J, Lyon B, Pershing A, Stancioff E, Jacobson GL (2020) Maine's climate future: 2020 update. Climate Change Institute Faculty Scholarship. 6. [https://digitalcommons.library.umaine.edu/climate\\_facpub/6](https://digitalcommons.library.umaine.edu/climate_facpub/6)

Fien EKP, Fraver S, Teets A, Weiskittel AR, Hollinger DY (2019) Drivers of individual tree growth and mortality in an uneven-aged, mixed-species conifer forest. *For Ecol Manage*. <https://doi.org/10.1016/j.foreco.2019.06.043>

Flanagan LB, Nikkel DJ, Scherloski LM, Tkach RE, Smits KM, Selinger LB, Rood SB (2021) Multiple processes contribute to methane emission in a riparian cottonwood forest ecosystem. *New Phytol* 229:1970–1982. <https://doi.org/10.1111/nph.16977>

Frazer GW, Canham CD, Lertzman KP (1999) Gap Light Analyzer (GLA), Version 2.0: Imaging software to extract canopy structure and gap light transmission indices from true-colour fisheye photographs, users manual and program documentation.

Gauci V, Gowing DJG, Hornibrook ERC, Davis JM, Dise NB (2010) Woody stem methane emission in mature wetland alder trees. *Atmos Environ* 44:2157–2160

Gauci V, Pangala SR, Shenkin A, Barba J, Bastviken D, Figueiredo V, Gomez C, Enrich-Prast A, Sayer E, Stauffer T, Welch B, Elias D, McNamara N, Allen M, Malhi Y (2024) Global atmospheric methane uptake by upland tree woody surfaces. *Nature* 631:796–800. <https://doi.org/10.1038/s41586-024-07592-w>

Gavlak RG, HDA, & MRO (2005) Soil pH and electrical conductivity. In: Plant, soil and water reference methods for the western region, 3rd edn. pp 37–47.

Harada M, Endo A, Wada S, Watanabe T, Epron D, Asakawa S (2024) Ubiquity of methanogenic archaea in the trunk of coniferous and broadleaved tree species in a mountain forest. *Antonie Van Leeuwenhoek* 117:107. <https://doi.org/10.1007/s10482-024-02004-5>

Hietala AM, Dörsch P, Kvaalen H, Solheim H (2015) Carbon dioxide and methane formation in Norway spruce stems infected by white-rot fungi. *Forests* 6:3304–3325. <https://doi.org/10.3390/f6093304>

Jeffrey LC, Maher DT, Chiri E, Leung PM, Nauer PA, Arndt SK, Tait DR, Greening C, Johnston SG (2021) Bark-dwelling methanotrophic bacteria decrease methane emissions from trees. *Nat Commun*. <https://doi.org/10.1038/s41467-021-22333-7>

Jeffrey LC, Moras CA, Tait DR, Johnston SG, Call M, Sippo JZ, Jeffrey NC, Laicher-Edwards D, Maher DT (2023)

Large methane emissions from tree stems complicate the wetland methane budget. *J Geophys Res Biogeosci* 128:e2023JG007679. <https://doi.org/10.1029/2023JG007679>

Kirschke S, Bousquet P, Ciais P, Saunois M, Canadell JG, Dlugokencky EJ, Bergamaschi P, Bergmann D, Blake DR, Bruhwiler L, Cameron-Smith P, Castaldi S, Chevallier F, Feng L, Fraser A, Heimann M, Hodson EL, Houweling S, Josse B, Fraser PJ, Krummel PB, Lamarque J-F, Langenfelds RL, Le Quéré C, Naik V, O'Doherty S, Palmer PI, Pison I, Plummer D, Poulter B, Prinn RG, Rigby M, Ringeval B, Santini M, Schmidt M, Shindell DT, Simpson JJ, Spahni R, Steele LP, Strode SA, Sudo K, Szopa S, van der Werf GR, Voulgarakis A, van Weele M, Weiss RF, Williams JE, Zeng G (2013) Three decades of global methane sources and sinks. *Nat Geosci* 6:813–823. <https://doi.org/10.1038/ngeo1955>

Klaus M, Öquist M, Macháčová K (2024) Tree stem-atmosphere greenhouse gas fluxes in a boreal riparian forest. *Sci Total Environ* 954:176243

Koschorreck M, Conrad R (1993) Oxidation of atmospheric methane in soil: measurements in the field, in soil cores and in soil samples. *Glob Biogeochem Cycles* 7:109–121

Kursa MB, Rudnicki WR (2010) Feature selection with the boruta package. *J Stat Softw* 36:1–13. <https://doi.org/10.18637/jss.v036.i11>

Liu L, Zhuang Q, Oh Y, Shurpali NJ, Kim S, Poulter B (2020) Uncertainty quantification of global net methane emissions from terrestrial ecosystems using a mechanistically based biogeochemistry model. *J Geophys Res Biogeosci* 125:e2019JG005428. <https://doi.org/10.1029/2019JG005428>

Machacova K, Papen H, Kreuzwieser J, Rennenberg H (2013) Inundation strongly stimulates nitrous oxide emissions from stems of the upland tree *Fagus sylvatica* and the riparian tree *Alnus glutinosa*. *Plant Soil* 364:287–301. <https://doi.org/10.1007/s11104-012-1359-4>

Maier M, Machacova K, Lang F, Svobodova K, Urban O (2018) Combining soil and tree-stem flux measurements and soil gas profiles to understand CH<sub>4</sub> pathways in *Fagus sylvatica* forests. *J Plant Nutr Soil Sci* 181:31–35. <https://doi.org/10.1002/jpln.201600405>

Martinez M, Ardón M, Carmichael MJ (2022) Identifying sources and oxidation of methane in standing dead trees in freshwater forested wetlands. *Front Environ Sci*. <https://doi.org/10.3389/fenvs.2021.737379>

Moisan MA, Lajoie G, Constant P, Martineau C, Maire V (2024) How tree traits modulate tree methane fluxes: a review. *Sci Total Environ*. <https://doi.org/10.1016/j.scitenv.2024.173730>

Nickerson N (2016) Evaluating gas emission measurements using Minimum Detectable Flux (MDF). <https://doi.org/10.13140/RG.2.1.4149.2089>

Oberle B, Covey KR, Dunham KM, Hernandez EJ, Walton ML, Young DF, Zanne AE (2018) Dissecting the effects of diameter on wood decay emphasizes the importance of cross-stem conductivity in *Fraxinus americana*. *Ecosystems* 21:85–97. <https://doi.org/10.1007/s10021-017-0136-x>

Pangala SR, Moore S, Hornibrook ERC, Gauci V (2013) Trees are major conduits for methane egress from tropical forested wetlands. *New Phytol* 197:524–531. <https://doi.org/10.1111/nph.12031>

Pangala SR, Hornibrook ERC, Gowing DJ, Gauci V (2015) The contribution of trees to ecosystem methane emissions in a temperate forested wetland. *Glob Chang Biol* 21:2642–2654. <https://doi.org/10.1111/gcb.12891>

Pinheiro J, Bates D, DebRoy S, Sarkar D, R Core Team (2021) *nlme: Linear and Nonlinear Mixed Effects Models*.

Pitz S, Megonigal JP (2017) Temperate forest methane sink diminished by tree emissions. *New Phytol* 214(4):1432–1439

Pitz SL, Megonigal JP, Chang CH, Szlavecz K (2018) Methane fluxes from tree stems and soils along a habitat gradient. *Biogeochemistry* 137:307–320. <https://doi.org/10.1007/s10533-017-0400-3>

Posit Team (2024) RStudio: Integrated Development Environment for R.

Putkinen A, Siljanen HMP, Laihonen A, Paasikoski I, Porkka K, Tirola M, Haikarainen I, Tenhovirta S, Pihlatie M (2021) New insight to the role of microbes in the methane exchange in trees: evidence from metagenomic sequencing. *New Phytol* 231:524–536

R Core Team (2024) R: A language and environment for statistical computing.

Read Z, Fraver S, D'Amato AW, Evans DM, Evans K, Lutz DA, Woodall CW (2023) CO<sub>2</sub> flux from *Acer saccharum* logs: sources of variation and the influence of silvicultural treatments. *Can J for Res* 53:654–662. <https://doi.org/10.1139/cjfr-2022-0291>

Reeburgh WS (2006) 4.03 Global Methane Biogeochemistry.

Rusch H, Rennenberg H (1998) Black alder (*Alnus glutinosa* (L.) Gaertn.) trees mediate methane and nitrous oxide emission from the soil to the atmosphere. *Plant Soil* 201:1–7. <https://doi.org/10.1023/A:1004331521059>

Saunois M, Bousquet P, Poulter B, Pergon A, Ciais P, Canadell JG, Dlugokencky EJ, Ettorre G, Bastviken D, Houweling S, Janssens-Maenhout G, Tubiello FN, Castaldi S, Jackson RB, Alexe M, Arora VK, Beerling DJ, Bergamaschi P, Blake DR, Brailsford G, Brovkin V, Bruhwiler L, Crevoisier C, Crill P, Covey K, Curry C, Frankenberg C, Gedney N, Höglund-Isaksson L, Ishizawa M, Ito A, Joos F, Kim HS, Kleinen T, Krummel P, Lamarque JF, Langenfelds R, Locatelli R, Machida T, Maksyutov S, McDonald KC, Marshall J, Melton JR, Morino I, Naik V, O'Doherty S, Parmentier FJW, Patra PK, Peng C, Peng S, Peters GP, Pison I, Prigent C, Prinn R, Ramonet M, Riley WJ, Saito M, Santini M, Schroeder R, Simpson JJ, Spahni R, Steele P, Takizawa A, Thornton BF, Tian H, Tohjima Y, Viovy N, Voulgarakis A, Van Weele M, Van Der Werf GR, Weiss R, Wiedinmyer C, Wilton DJ, Wiltshire A, Worthy D, Wunch D, Xu X, Yoshida Y, Zhang B, Zhang Z, Zhu Q (2016) The global methane budget 2000–2012. *Earth Syst Sci Data* 8:697–751. <https://doi.org/10.5194/essd-8-697-2016>

Saunois M, Stavert AR, Poulter B, Bousquet P, Canadell JG, Jackson RB, Raymond PA, Dlugokencky EJ, Houweling S, Patra PK, Ciais P, Arora VK, Bastviken D, Bergamaschi P, Blake DR, Brailsford G, Bruhwiler L, Carlson KM, Carroll M, Castaldi S, Chandra N, Crevoisier C, Crill PM, Covey K, Curry CL, Ettorre G, Frankenberg C, Gedney N, Hegglin MI, Höglund-Isaksson L, Hugelius

G, Ishizawa M, Ito A, Janssens-Maenhout G, Jensen KM, Joos F, Kleinert T, Krummel PB, Langenfelds RL, Laruelle GG, Liu L, Machida T, Maksyutov S, McDonald KC, McNorton J, Miller PA, Melton JR, Morino I, Müller J, Murguia-Flores F, Naik V, Niwa Y, Noce S, O'Doherty S, Parker RJ, Peng C, Peng S, Peters GP, Prigent C, Prinn R, Ramonet M, Regnier P, Riley WJ, Rosentreter JA, Segers A, Simpson IJ, Shi H, Smith SJ, Steele LP, Thornton BF, Tian H, Tohjima Y, Tubiello FN, Tsuruta A, Viovy N, Voulgarakis A, Weber TS, van Weele M, van der Werf GR, Weiss RF, Worthy D, Wunch D, Yin Y, Yoshida Y, Zhang W, Zhang Z, Zhao Y, Zheng B, Zhu Q, Zhu Q, Zhuang Q (2020) The global methane budget 2000–2017. *Earth Syst Sci Data* 12:1561–1623. <https://doi.org/10.5194/essd-12-1561-2020>

Shoemaker JK, Keenan TF, Hollinger DY, Richardson AD (2014) Forest ecosystem changes from annual methane source to sink depending on late summer water balance. *Geophys Res Lett* 41:673–679. <https://doi.org/10.1002/2013GL058691>

Sjögersten S, Siegenthaler A, Lopez OR, Aplin P, Turner B, Gauci V (2020) Methane emissions from tree stems in neotropical peatlands. *New Phytol* 225:769–781. <https://doi.org/10.1111/nph.16178>

Terazawa K, Yamada K, Ohno Y, Sakata T, Ishizuka S (2015) Spatial and temporal variability in methane emissions from tree stems of *Fraxinus mandshurica* in a cool-temperate floodplain forest. *Biogeochemistry* 123:349–362. <https://doi.org/10.1007/s10533-015-0070-y>

Vainio E, Haikarainen IP, Machacova K, Putkinen A, Santalahti M, Koskinen M, Fritze H, Tuomivirta T, Pihlatie M (2022) Soil-tree-atmosphere CH<sub>4</sub> flux dynamics of boreal birch and spruce trees during spring leaf-out. *Plant Soil* 478:391–407. <https://doi.org/10.1007/s11104-022-05447-9>

van Haren J, Brewer PE, Kurtzberg L, Wehr RN, Springer VL, Espinoza RT, Ruiz JS, Cadillo-Quiroz H (2021) A versatile gas flux chamber reveals high tree stem CH<sub>4</sub> emissions in Amazonian peatland. *Agric For Meteorol*. <https://doi.org/10.1016/j.agrformet.2021.108504>

von Fischer JC, Hedin LO (2007) Controls on soil methane fluxes: tests of biophysical mechanisms using stable isotope tracers. *Glob Biogeochem Cycles*. <https://doi.org/10.1029/2006GB002687>

Wang Z-P, Gu Q, Deng F-D, Huang J-H, Megonigal JP, Yu Q, Lü X-T, Li L-H, Chang S, Zhang Y-H, Feng J-C, Han X-G (2016) Methane emissions from the trunks of living trees on upland soils. *New Phytol* 211:429–439

Warner DL, Villarreal S, McWilliams K, Inamdar S, Vargas R (2017) Carbon dioxide and methane fluxes from tree stems, coarse woody debris, and soils in an upland temperate forest. *Ecosystems* 20:1205–1216. <https://doi.org/10.1007/s10021-016-0106-8>

Yip DZ, Veach AM, Yang ZK, Cregger MA, Schadt CW (2019) Methanogenic *Archaea* dominate mature heartwood habitats of Eastern Cottonwood (*Populus deltoides*). *New Phytol* 222:115–121. <https://doi.org/10.1111/nph.15346>

**Publisher's Note** Springer Nature remains neutral with regard to jurisdictional claims in published maps and institutional affiliations.